Analytical model of electric field assisted ion diffusion into glass containing two indigenous mobile species, with application to poling

R. Oven

School of Engineering, University of Kent,

Canterbury, CT2 7NT, UK

Abstract

An analytical model of electric field assisted diffusion of ions into glass is extended to include two indigenous mobile ion species that are initially uniformly distributed within the glass. A quasi-stationary state solution that includes diffusion effects and is applicable when the invasive ions have a lower mobility than the two indigenous species is presented. It is relevant to the electrical poling of soda-lime and borosilicate glasses with concentrations of mobile ions (Na^+, K^+) that are processed with a non-blocking anode where hydrogen ion injection occurs. The model is compared with numerical solutions based on the drift-diffusion equations and Poisson's equation and shows good agreement. The increase in the concentration of the indigenous species with the lower mobility (K^+) below the poled layer within a pile-up region is accurately modelled.

Key words field assisted diffusion; poling;

I. INTRODUCTION

The number of potential applications of electrically poled glass has widened considerably in the literature in recent years. These include its use as a non-linear optical material [1-5] and as a layer in order to produce buried or surface channel optical waveguides [6-11]. The difference in refractive index between poled and un-poled glass has been used to make diffractive phase masks [12,13]. Electrical poling has also be used in a process to control the size of metallic nanoparticles in glass in an image replication using a bleaching process [12]. The compaction of a poled glass layer relative to an un-poled one has been used to produce nano-surface profile features in glass [14, 15]. Changing the surface properties of bio-active glasses by electrical poling has also been investigated [16-19]. The control of the surface reactivity of poled borosilicate glass has also suggested its use as a smart substrate [20]. Finally, the removal of ions by glass poling can result in a reduction in loss and permittivity at microwave frequencies [21].

It is well known that the ion transport processes that occur during poling of glass is dependent upon the nature of the anode used during the process, which at the extremes can be either blocking or non-blocking [22-24]. A blocking anode does not result in the injection of any ions into the glass. As a result when a high voltage is applied at elevated temperature, mobile cations (typically Na^+, K^+, Ca^{++}) are removed from the region of glass directly below the anode. As a consequence a negative space charge and high electric field develop in the depletion region. This high field can cause the motion of the negatively charged non-bridging oxygen ions towards the anode [23, 5]. It has also been suggested that for some glasses, if the field in the depletion region reaches the breakdown field then electronic motion is also possible

[19]. The rate at which the depletion region growth slows with time and eventually stops since most of the applied potential is dropped across it [5].

For non-blocking anodes the situation is different as this type allows the field assisted injection of low mobility hydrogen or hydronium ions (H_3O^+) from the atmosphere into the glass. This is similar to a field assisted ion exchange processes with the injection of low mobility ions, which replace the indigenous ions in the near surface region [25, 5]. In comparison to a blocking anode, the poled glass region for this type of anode can be deeper since the poling current is greater for a longer time [5].
For both blocking and non-blocking anodes, indigenous lower mobility ions can build up in the region below the poled glass layer. The extent to which this effect is significant depends on the processing temperature, which determines their mobility and the field present in the poled glass layer. For glasses containing K^+ ions, the pile-up region due to K^+ ion motion has been observed in chemical and refractive index profiles [2, 4, 7-8,13, 26].

The blocking anode case has been analysed analytically by ignoring diffusion effects but considering ion drift motion together with Poisson's equation to model the space charge formation [25]. The modelling did not consider oxygen ion or electronic motion or field dependent mobility effects but was compared with numerical simulations based on ion drift and diffusion equations coupled with Poisson equation. An alternative analysis, which considered oxygen ion drift motion in a developed depletion region, was recently considered using a numerical approach [5].

The modelling of the poling process with a non-blocking anode has also been considered in the literature by applying an analytical model developed for field assisted ion exchange by Prieto and Linares [27]. This model is applicable to a glass with a single mobile ion species where the sample voltage is constant. In such a case, the total ion current reduces with time and the diffusion front between the injected and indigenous ions broadens due to diffusion effects. This results in a so called quasi-stationary state concentration profile forming for the invasive ions. This simple model has been used to discuss poling experiments with non-blocking anodes [5,12, 29-30]. One limitation of this model is that the glass is assumed to have only one indigenous ion species and so the pile-up of lower mobility ions mentioned above is not modelled despite being experimentally observed. In a number of the above applications, a knowledge of the time evolution of the piled-up ion concentration profile is desirable. This is obvious in optical waveguide applications where the refractive index profile of the pile-up region forms the guide [7]. Another application where the pile-up effect is important is in the formation of surface relief profiles, for although the relief profile in poled glass is attributed to the compaction of the poled layer, it is well known that the replacement of Na^+ ions by K^+ ions in an ion-exchange results in a volume expansion [14, 15, 28]. Hence, the surface relief formed in poled glass should be a result of the difference in poled glass compaction countered by a corresponding expansion of the underlying K^+ pile-up region.

The modelling of the poling process with a non-blocking anode has also been performed numerically based on ion drift and diffusion equations coupled with Poisson's equation. However, no analytical model that includes diffusion effects has been reported [25]. In this paper, we consider the non-blocking anode case

analytically where the glass has two indigenous mobile ion species. We derive quasi-stationary analytical solutions when the invasive ion species has a lower mobility than the two indigenous species. This results in a pile-up of the indigenous species with the lower mobility below the exchanged layer. The analytical results are compared with numerical calculations with parameters applicable to the electrically poling from a non-blocking electrode into borosilicate glass that has Na^+ and K^+ ions present. In order to make the results relevant to experimental situations commonly encountered, we consider the case where the processing is performed with a voltage source that necessitates the application of the quasi-stationary state approach [27], which is an extension to the constant current stationary state approach [31].

II. MODEL

II.1 First order model

Following previous work on deriving a quasi-stationary state profile with just one indigenous species, we first consider the exchange process without diffusion effects in order to establish approximate expressions for the total ion flux $j(t)$ as a function of time and the diffusion front velocities [27]. In the next section we then include diffusion effects. We consider a quasi-neutral model where we ignore space charge effects. The appropriateness of this approximation to field assisted ion exchange with a glass with a single ion species has previously been confirmed analytically and has been discussed previously [32]. For glass like silica the mobile ion concentrations are small and space charge regions can extend over significant distances [25]. However, in soda-lime and borosilicate glasses the mobile ion concentrations are large so the distances over which space charges extend are very small, hence the space charge neutral approximation is valid. The validity of this approximation will also be shown

by comparing our solutions to numerical solutions that include the possibility of space charge build-up.

Figure 1 shows the process and the associated step-like ion profiles that will develop when diffusion effects are ignored. We consider H^+ ions being injected from the anode into a glass that contains Na^+ and K^+ ions that are initially uniformly distributed. The H^+ ions have a lower mobility than the Na^+ and K^+ ions. Due to their lower mobility, the H ions form a step profile of depth d_1. The K^+ ions have a lower mobility than the Na^+ ions, hence the K^+ ions will form a pile-up region of thickness $(d_2\text{-}d_1)$ just below the H^+ ion exchange region. The glass will hence be divided into three regions with electric fields E_i that are constant in each region.

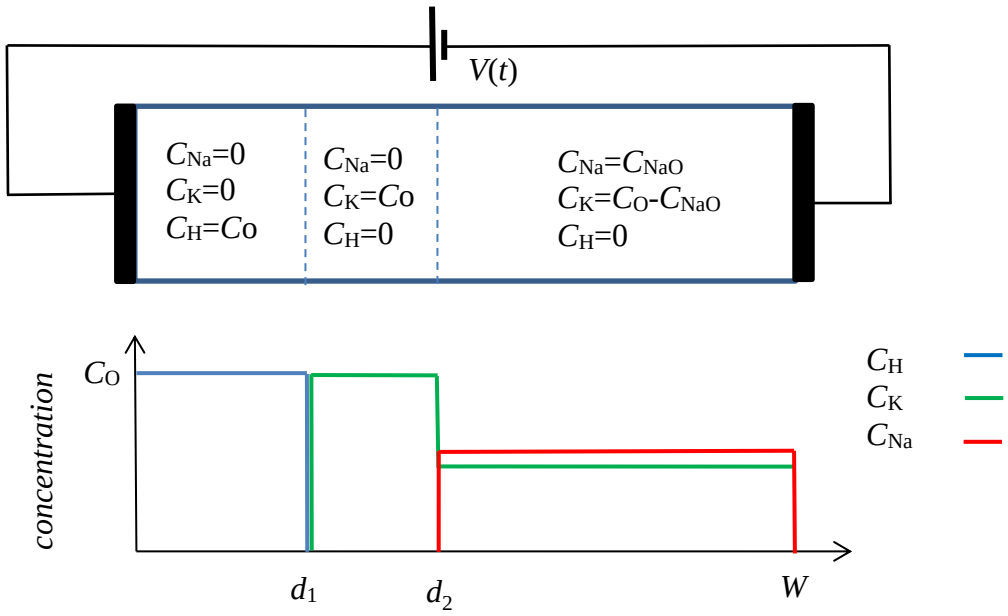

Fig.1 Field assisted diffusion – first order model ignoring diffusion effects. Diffusion fronts indicated by dotted lines. (Colour on-line)

If μ_m is the mobility of the m^{th} ion type and W is the glass thickness then the following equations are applicable

$$d_1E_1 + (d_2 - d_1)E_2 + (W - d_2)E_3 = V(t) \tag{1}$$

$$j(t) = \mu_H C_O E_1 = \mu_K C_O E_2 = (\mu_{Na} C_{NaO} + \mu_K C_{KO})E_3 \tag{2}$$

$$\frac{dd_1}{dt} = \mu_H E_1 = \frac{j(t)}{C_O} \tag{3}$$

$$\frac{dd_2}{dt} = \mu_{Na} E_3 = \frac{\mu_{Na}}{\mu_{Na} C_{NaO} + \mu_K C_{KO}} . j(t) \tag{4}$$

In these equations C_{NaO} and C_{KO} are the Na^+ and K^+ ion concentrations in the bulk of the glass and $C_O = C_{NaO} + C_{KO}$ is the total mobile ion concentration. We assume for generality that the supply voltage V(t) is time dependant; which can be the case in real poling experiments. Integrating (3) and (4), with $d_1(0)=0$ and $d_2(0)=0$, gives

$$d_1(t) = \frac{1}{C_O} \int_0^t j(u)du \tag{5}$$

and

$$d_2(t) = \frac{\mu_{Na}}{\mu_{Na} C_{NaO} + \mu_K C_{KO}} \int_0^t j(u)du \tag{6}$$

Hence from (5) and (6), d_1 and d_2 are related via

$$\frac{d_2(t)}{d_1(t)} = \frac{C_O \mu_{Na}}{C_{NaO} \mu_{Na} + C_{KO} \mu_K} \tag{7}$$

It can be seen from (3) and (4) that the diffusion fronts for H^+ and Na^+ ions d_1 and d_2 are moving in the glass with different velocities, hence quasi-stationary state solutions for these two ion species are to be expected. Equation (7) shows the two fronts maintain a fixed ratio so the K^+ ion profile in not quasi-stationary.

From eqn. (1-5) it is also possible to show that the time dependence of the ion flux is given by

$$j(t) = \frac{(\mu_{Na} C_{NaO} + \mu_K C_{KO}) V(t)}{\sqrt{W^2 + 2a\mu_H \int_0^t V(u)du}} \tag{8}$$

where

$$a = \left(\frac{\mu_{Na} C_{NaO} + \mu_K C_{KO}}{\mu_H C_O}\right)^2 - \frac{\mu_{Na}}{\mu_H} + \frac{(\mu_{Na} - \mu_K) C_{KO}}{\mu_K C_O}\left(\frac{\mu_{Na} C_{NaO} + \mu_K C_{KO}}{\mu_H C_O}\right) \tag{9}$$

If $\mu_K \rightarrow 0$ and $C_{KO} \rightarrow 0$ then (8) and (9) reduce to the expressions for a glass with a single ion type [27].

II.2 Quasi stationary state solutions

In this section analytical expressions for the quasi-stationary state concentration profiles including diffusion effects are derived. We first derive the coupled drift diffusion equations for H^+ and Na^+ ions since these will have quasi-stationary solutions. In general the three ion fluxes, j_m, are given by

$$j_m = \mu_m E C_m - D_m \frac{\partial C_m}{\partial x} \qquad m = Na, K, H \tag{10}$$

where E is the electric field, D_m is the diffusion coefficient and μ_m is the ion mobility. D_m and μ_m are related by

$$\frac{D_m}{\mu_m} = \frac{HkT}{q} \tag{11}$$

where H is the Haven ratio. Following the quasi-neutral approach we assume the ion species are coupled by a space charge neutrality condition

$$C_{Na} + C_K + C_H = C_{Nao} + C_{Ko} = C_o \tag{12}$$

This approximation has been shown to be valid in a previous study for glasses with a high mobile ion concentration [32]. As a consequence of (12), total ion flux, $j(t)$, is a constant independent of position.

$$j(t) = j_{Na} + j_K + j_H \tag{13}$$

The continuity equations for Na^+ and H^+ ions are

$$-\frac{\partial j_m}{\partial x} = \frac{\partial C_m}{\partial t} \quad (m = Na, H) \tag{14}$$

Combining eqn. (10-14) gives the electric field with diffusion terms

$$E = \frac{j(t) + (D_H - D_K)\frac{\partial C_H}{\partial x} + (D_{Na} - D_K)\frac{\partial C_{Na}}{\partial x}}{(\mu_H - \mu_K)C_H + (\mu_{Na} - \mu_K)C_{Na} + \mu_K C_O} \tag{15}$$

Substituting eqns. (15) and (10) into (14) gives two coupled PDEs

$$\frac{\partial C_m}{\partial t} = -D_m \frac{\partial}{\partial x}\left\{\frac{j(t)C_m}{(D_m - D_K)C_m + (D_n - D_K)C_n + C_O D_K}\right\}$$
$$+ D_m \frac{\partial}{\partial x}\left\{\frac{(D_n - D_K)\left[C_n \frac{\partial C_m}{\partial x} - C_m \frac{\partial C_n}{\partial x}\right] + C_O D_K \frac{\partial C_m}{\partial x}}{(D_m - D_K)C_m + (D_n - D_K)C_n + C_O D_K}\right\}$$

(16)

where (*m*,*n*) = (Na, H) or (H, Na). The two equations of (16) are in general coupled. However, once the piled-up K^+ ion region is established and becomes wide enough in comparison to any diffusional smearing of the ion profiles, the two equations will become uncoupled. In terms of concentration profiles $C_{Na} = 0$ in regions where C_H is non-zero and likewise $C_H = 0$ in regions where C_{Na} is non-zero. Under these conditions the term in square brackets in (16) is zero and hence (16) becomes uncoupled

$$\frac{\partial C_m}{\partial t} = -\frac{D_m D_K C_O j(t)}{[(D_m - D_K)C_m + C_O D_K]^2}\frac{\partial C_m}{\partial x} + D_m \frac{\partial}{\partial x}\left\{\frac{C_O D_K}{(D_m - D_K)C_m + C_O D_K}\frac{\partial C_m}{\partial x}\right\}$$

(17)

where *m* =Na or H. Physically, this implies that the H^+ ions are locally being driven into a glass of composition determined solely by K^+ ions of concentration C_O and that the Na^+ ions are locally moving in a glass of composition determined by the Na^+ and K^+ ions.

Following the quasi stationary approach of Prieto and Linares we now change to a moving frame of reference [27]. However, in this work the moving frame will be different for the Na^+ and H^+ ion rich regions as suggested by the non-diffusive model in the previous section. From eqn. (5) for the H^+ ions we use

$$x_H = x - \frac{1}{C_O}\int_0^t j(u)du$$

(18)

and from eqn. (6) for the Na^+ ions we use

$$x_{Na} = x - \frac{\mu_{Na}}{\mu_{Na}C_{NaO} + \mu_K C_{KO}} \int_0^t j(u)du \tag{19}$$

We also perform changes to dimensionless space and time variables

$$z_{Na} = \frac{j(t)x_{Na}}{C_O D_{Na}}, \qquad z_H = \frac{j(t)x_H}{C_O D_{Na}}, \quad \tau = \frac{1}{C_O^2 D_{Na}} \int_0^t j^2(u)du \tag{20}$$

to give

$$\frac{\partial C_H}{\partial \tau} = \left\{ -\frac{D_{Na}{C_O}^2}{j^3}\frac{dj}{dt} z_H - \frac{M_H M_K {C_O}^2}{[(M_H - M_K)C_H + M_K C_O]^2} + 1 \right\} \frac{\partial C_H}{\partial z_H} + \frac{\partial}{\partial z_H}\left\{ \frac{M_H M_K C_O}{(M_H - M_K)C_H + M_K C_O} . \frac{\partial C_H}{\partial z_H} \right\} \tag{21}$$

and

$$\frac{\partial C_{Na}}{\partial \tau} = \left\{ -\frac{D_{Na}{C_O}^2}{j^3}\frac{dj}{dt} z_{Na} + \frac{M_K {C_O}^2}{[(1 - M_K)C_{Na} + M_K C_O]^2} + \frac{C_O}{C_{Nao} + M_K C_{Ko}} \right\} \frac{\partial C_{Na}}{\partial z_{Na}} + \frac{\partial}{\partial z_{Na}}\left\{ \frac{M_K C_O}{(1 - M_K)C_{Na} + M_K C_O} . \frac{\partial C_{Na}}{\partial z_{Na}} \right\} \tag{22}$$

where M_m is the mobility ratio

$$M_m = \frac{\mu_m}{\mu_{Na}} = \frac{D_m}{D_{Na}} \tag{23}$$

We now apply the quasi-stationary state approximation by assuming that $j(t)$ varies slowly enough such that the first terms on the *r.h.s.* of (21) and (22) can be neglected [27]. Using (8), these terms can be neglected in relation to the third terms on the *r.h.s.* of (21) if

$$\frac{HkT}{qV}\frac{C_0^2|z_H|aM_H}{(C_{NaO}+M_KC_{KO})^2} \ll 1$$

(24)

Likewise for eqn. (22).

$$\frac{HkT}{qV}\frac{C_O|z_{Na}|aM_H}{(C_{NaO}+M_KC_{KO})} \ll 1$$

(25)

We assume here that these inequalities apply and justify them in Appendix 1.

Stationary state solutions to (21) and (22) of the form $C_{Na}(\eta_{Na})$ and $C_H(\eta_H)$ are now assumed where

$$\eta_m = z_m - \nu_m\tau$$

(26)

so $\frac{\partial C_m}{\partial z_m} = \frac{dC_m}{d\eta_m}$ and $\frac{\partial C_m}{\partial \tau} = -\nu_m\frac{dC_m}{d\eta_m}$. These transformations reduce (21) and (22) to the ordinary differential equations

$$-\nu_H\frac{dC_H}{d\eta_H} = \left\{1 - \frac{M_KM_HC_O{}^2}{[(M_H-M_K)C_H+M_KC_O]^2}\right\}\frac{dC_H}{d\eta_H} + \frac{d}{d\eta_H}\left\{\frac{M_KM_HC_O}{(M_H-M_K)C_H+M_KC_O}\cdot\frac{dC_H}{d\eta_H}\right\}$$

(27)

and

$$-\nu_{Na}\frac{dC_{Na}}{d\eta_{Na}} = \left\{\frac{C_O}{C_{NaO}+M_KC_{KO}} + \frac{M_KC_O{}^2}{[(1-M_K)C_{Na}+M_KC_O]^2}\right\}\frac{dC_{Na}}{d\eta_{Na}} + \frac{d}{d\eta_{Na}}\left\{\frac{M_KC_O}{(1-M_K)C_{Na}+M_KC_O}\cdot\frac{dC_{Na}}{d\eta_{Na}}\right\}$$

(28)

These may be integrated with the following boundary conditions

$$C_{Na} = 0\,, \frac{dC_{Na}}{d\eta_{Na}} = 0 \; as \; \eta_{Na} \to -\infty, C_{Na} = C_{NaO}, \frac{dC_{Na}}{d\eta_{Na}} = 0 \; as \; \eta_{Na} \to +\infty$$

(29)

and

$$C_H = \; C_O, \frac{dC_H}{d\eta_H} = 0 \; as \; \eta_H \to -\infty, \; C_H = 0\,, \frac{dC_H}{d\eta_H} = 0 \; as \; \eta_H \to +\infty$$

(30)

which give both velocities $v_{Na} = 0$ and $v_H = 0$ and show that the transformations used, namely (18) and (19), were appropriate for the two diffusion fronts. Assuming $C_H(\eta_H=0) = C_O/2$ and $C_{Na}(\eta_{Na}=0) = C_{NaO}/2$ as approximate initial conditions for the solution and transforming back to the (x, t) co-ordinates finally gives

$$C_H(x,t) = \frac{C_O}{1 + exp\left(\frac{M_K - M_H}{M_K M_H} . \frac{j(t)}{D_{Na} C_O}\left(x - \frac{1}{C_O}\int_0^t j(u)\, du\right)\right)}$$

(31)

and

$$C_{Na}(x,t) = \frac{C_{NaO}}{1 + exp\left(-\frac{(1 - M_K)C_{NaO}}{(C_{NaO} + M_K C_{KO})M_K} . \frac{j(t)}{D_{Na} C_O}\left(x - \frac{1}{C_{NaO} + M_K C_{KO}} . \int_0^t j(u)\, du\right)\right)}$$

(32)

where from (8) for a constant V

$$\int_0^t j\,(u) du = \frac{(C_{NaO} + M_K C_{KO})}{a M_H}\left(\sqrt{W^2 + 2a\mu_H V t} - W\right)$$

(33)

The analytical form for the H^+ profile, eqn. (31) is similar to that for the single ion model [27] but with a different constant involving the mobility ratios.

The K^+ ion profile $C_K(x,t)$ can be calculated from eqn. (12)

$$C_K(x,t) = C_o - C_{Na}(x,t) - C_H(x,t)$$

(34)

Hence the K^+ ion profile is not a simple quasi-stationary profile but involves two quasi-stationary profiles each moving with different velocities.

III. Comparison with numerical computations.

We compare the analytical expressions with numerical solutions of the drift-diffusion equations and Poisson's equations in order to confirm the space charge neutral assumption and the accuracy of the quasi-stationary approximation. Following ref. [25] we numerically solve

$$\frac{\partial C_m}{\partial t} + \mu_m \frac{\partial E C_m}{\partial x} = D_m \frac{\partial^2 C_m}{\partial x^2} \qquad m = Na, K, H$$

$$\frac{\partial E}{\partial x} = \frac{q(C_H + C_K + C_{Na} - C_0)}{\varepsilon_o \varepsilon_r}$$

(34)

with the initial and boundary conditions

$$C_H(0,t) = C_o, C_K(W,t) = C_{Ko}, C_{Na}(W,t) = C_{Nao}$$

$$C_H(x,0) = 0, C_K(x,0) = C_{Ko}, C_{Na}(x,0) = C_{Nao}, E(x,0) = \frac{V}{W}$$

(35)

We solve these numerically by using the MATLAB PDE toolbox with model parameters C_O= 6.8x10^{27}m^{-3} and C_{Nao}/C_O=0.605 and C_{Ko}/C_O =0.395 and ε_r= 5 which are typical of a borosilicate crown glass. We also assume a processing temperature of 400^{o}C, μ_{Na}=1.3x10^{-15} m^{2}V^{-1}s^{-1}, H=1, M_K=0.0125, M_H=0.001, V=100 V and W=1 mm. Figure 2 shows concentration profiles calculated from computer simulations and the analytical model eqns. (31) to (34) corresponding to a poling time of 3 hours. For this time it can be seen that the piled-up region of K^+ ions and hence also the quasi-

stationary profiles for Na^+ and H^+ ions are well established. It can be seen that the analytical profiles are in excellent agreement with the computer simulations. This confirms that for the typical processing parameters chosen the space charge neutral approximation and the quasi-stationary approximations are valid.

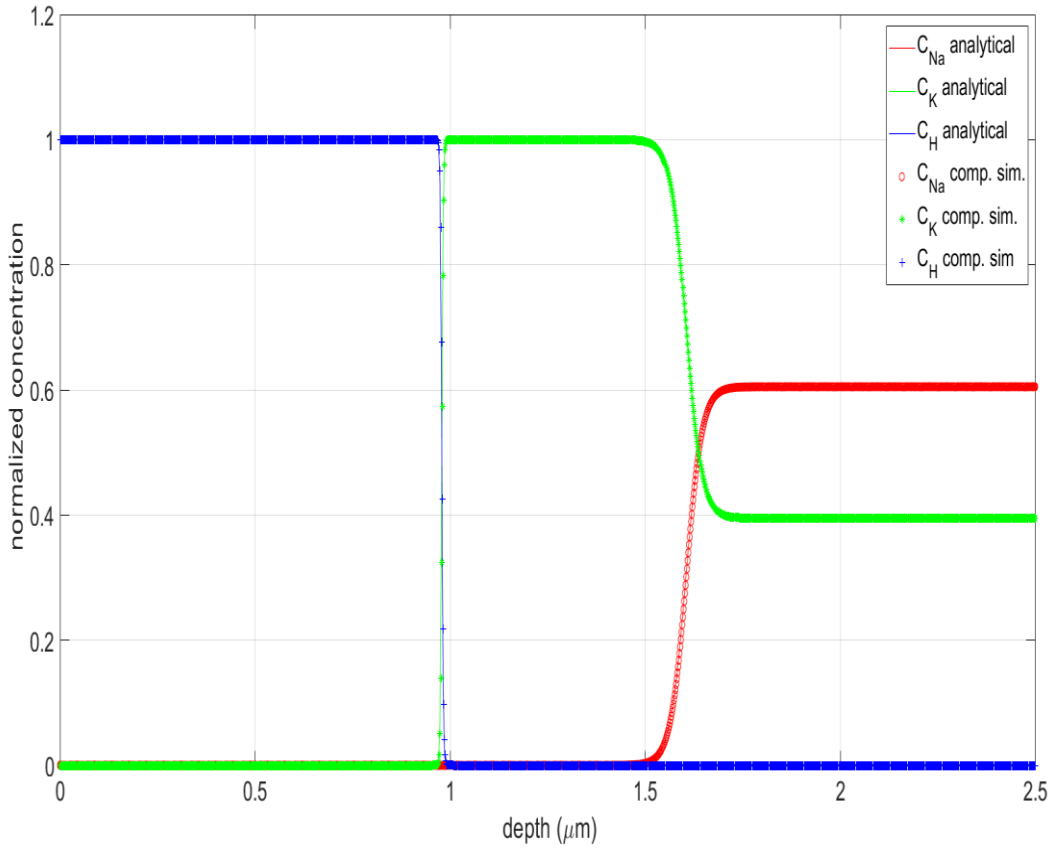

Fig 2 Comparison between analytical model and computer simulations. Parameters used are C_O= 6.8x10^{27}m^{-3}, C_{NaO}/C_O=0.605, C_{KO}/C_O =0.395, T= 400ºC, μ_{Na}=1.3x10^{-15} m^{2}V^{-1}s^{-1}, M_K=0.0125, M_H=0.001, V=150V and W=1 mm, t=3 hours. Concentrations normalized with respect to Co. For computer simulation ε_r= 5 was assumed. (Colour on-line)

From fig. 2 it can be seen that the leading (deeper) edge of the K^+ ion profile is wider than its trailing edge due to the back diffusion of the more mobile sodium ions against

the applied field, whilst the trailing edge is step-like since the back diffusion of K^+ ions into the H^+ region is less due to the lower diffusion coefficient of the K^+ ions. Further, the established K^+ pile-up region prevents Na^+ back diffusion into the H^+ region. Recent optical reflectivity measurements of leaky modes supported by poled soda-lime glass samples indicate a rapid almost abrupt (~10^{-4} μm) change in refractive index between the low refractive index of the poled glass and the higher refractive index of the underlying glass [33]. Using the model developed in this paper this would correspond to the H^+-K^+ transition in the profile.

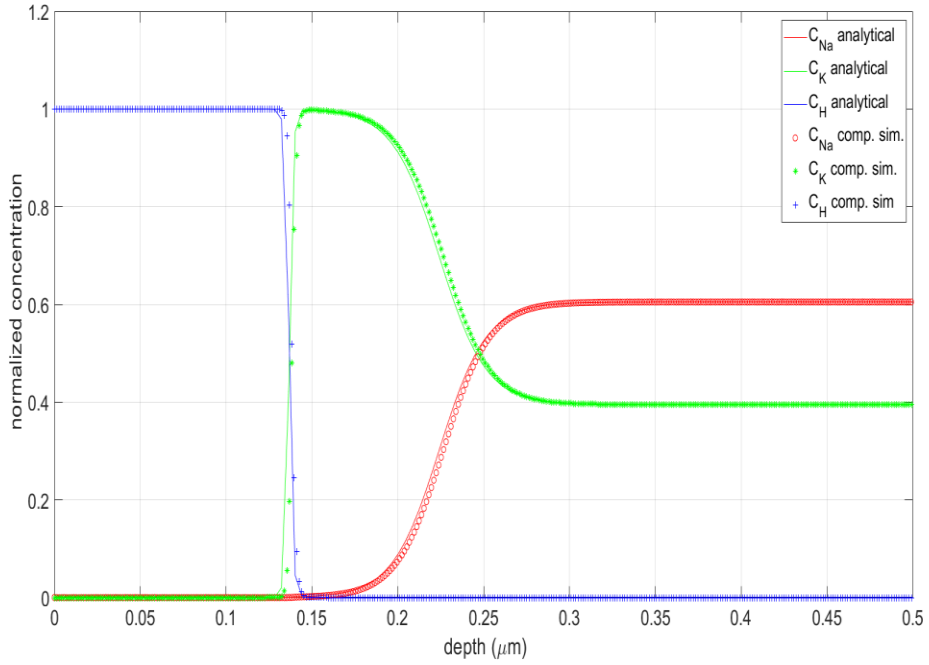

Fig 3 Comparison between analytical model and computer simulations. *V*=100V and *t*=30 min other parameters as for fig. 2 (Colour on-line). Concentrations normalized with respect to *C*o.

Figure 3 shows the analytical and computer simulation profiles for the same material parameters but for a lower voltage V=100V and for a shorter poling time of 30 min. It can be seen that even for these parameters the ion profiles have reached a quasi-stationary state. The resulting K^+ concentration profile transition is wider at the

leading (deeper) edge relative to the poling depth, indicating more significant diffusion relative to drift transport due to the lower field.

Figure 4 compares the sample current density $J(t) = qj(t)$ obtained from the numerical simulations with that obtained from the first order analytical model where $j(t)$ is given by eqn. (8) for the same parameters as for fig. 2. It can be seen that the two current density curves are in good agreement. The decay is mainly due to the increase in resistance of the glass due to the H^+ poled layer, as in a glass with a single ion species. It can be seen from eqn. (8) that the product $a\mu_H$ determines the decay rate of the current. From eqn. (9) with M_H~1/1000 and M_K~1/100 then

$$a \cong \left(\frac{C_{NaO} + M_K C_{KO}}{M_H C_O}\right)^2 \tag{36}$$

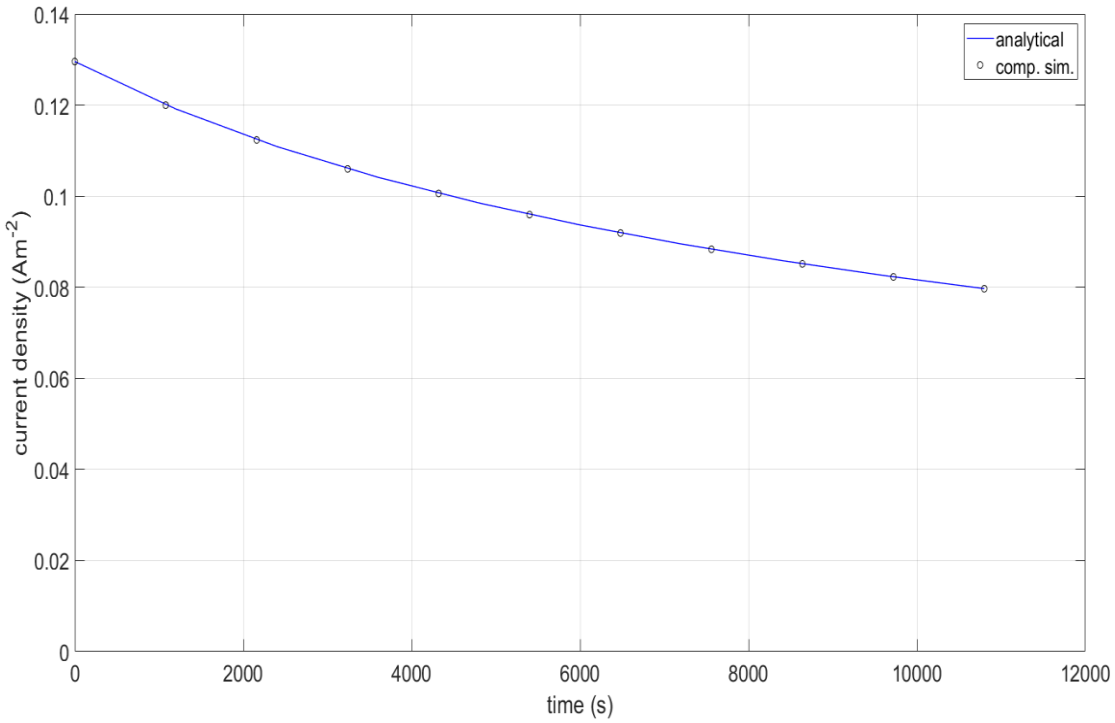

Fig. 4. Comparison between analytical model and computer simulations for current density, time data. Parameters same as for fig. 2. Analytical is solid curve, dots are computer simulation. (Colour on-line)

which may be further approximated, since M_K<<1, to $a \cong \left(\frac{C_{NaO}}{M_H C_O}\right)^2$. This is independent of M_K and only differs from that of the single indigenous ion model by the concentration ratio $(C_{Na0}/C_0)^2$. Hence, it is difficult to discern differences between the single and double indigenous ion models from the current-time data. However, this does suggest that the mobility of H^+ ions can be deduced from this data even for glasses with Na^+ and K^+ ions.

Limitations in using drift-diffusion models to analyse the poling of glasses with high concentrations of mobile ions have been discussed previously [25]. These include ignoring concentration dependent H^+ diffusion coefficients and the neglect of oxygen ion motion towards the surface. It is also worth noting that due to the high field values developed across the H^+ region, the H^+ ion mobility may in practice be field dependent [24, 34]. Although this work is an extension of previous models, [27], in that it includes K^+ ion motion and diffusion effects in an analytical model, the above limitations still apply to the poling of glass. Further, it does not consider divalent Ca^{++} ion motion. These have a lower mobility than H^+ ions and will not form a stationary profile and hence will necessitate numerical modelling [25].

The use of the boundary condition $C_H=C_0$ at the anode, which is used in this and other modelling requires some discussion. Second harmonic generation (SHG) in poled glass is normally attributed to a frozen-in space charge region associated with non-uniform ionic concentrations within the depletion region although there is some evidence of an ionic polarization mechanism [35]. Experiments show SHG is reduced

but still exists in samples produced with non-blocking, in comparison to blocking, anodes [5]. This suggests that complete space charge compensation by H^+ ions does not occur in all experimental situations for non-blocking anodes. In theory, for complete space-charge compensation by H^+ ions, the current density $J(t)$ during poling needs to be limited so the supply of H^+ at the anode matches that demanded by $J(t)$. When this is done experimentally, estimates suggest C_H can be close to C_0 [24].

IV. Conclusions

The quasi-stationary analytical model of electric field assisted diffusion of ions in glass has been extended to include glasses that have two indigenous mobile ion types. When the invasive ions (H^+) have a lower mobility than the two indigenous types (Na^+, K^+), the invasive ion profile and the ion profile of the fastest indigenous ion type evolve into quasi-stationary profiles. The indigenous ion with the lower mobility (K^+) forms a pile-up region in front of the advancing invasive ion front. The model has been compared with numerical solutions based on the drift-diffusion equations and Poisson's equation using parameters typically experienced in poling experiments using soda-lime or borosilicate glasses, which have a relatively high sodium ion concentration and shows excellent agreement. The pile-up of the indigenous ion with the lower mobility, below the exchanged layer is modelled well by the analytical expressions.

Appendix 1

The approximations (24) and (25) and hence the validity of the concentration profile formulas are considered [27]. We first consider the H^+ ion profile eqn. (31), C_H changes from $0.99C_0$ to $0.01C_0$ over a range of z_H given by

$$\frac{M_K - M_H}{M_K M_H}|z_H| \ll 4.6$$

(A1)

Substituting (A1) and (36) into (24) gives

$$\frac{HkT}{qV}\left[\frac{M_K}{M_K - M_H}\right] 4.6 \ll 1$$

(A2)

The term in brackets in eqn. (A2) is ~1 for $M_K >> M_H$ so for H=1, then at T=623 K, V >> 0.25 V for the quasi-stationary state to apply. For most poling experiments V >100 V so this inequality is easily met in practice.

For the Na ion profile eqn. (32), C_{Na} changes from $0.99C_{Na0}$ to $0.01C_{Na0}$ over a range of z_{Na} given by

$$\frac{(1 - M_K)C_{Na0}}{(C_{Na0} + C_{K0}M_K)M_K}|z_{Na}| \ll 4.6$$

(A3)

Substituting (36) and (A3) into (25) gives

$$\frac{HkT}{qV}\left[\frac{(C_{Na0} + M_K C_{K0})^2 M_K}{(1 - M_K)M_H C_0 C_{Na0}}\right] 4.6 \ll 1$$

(A4)

which for M_K<<1 approximates to

$$\frac{HkT}{qV}\left[\frac{C_{Na0}M_K}{M_H C_0}\right] 4.6 \ll 1$$

(A5)

hence for H=1, M_K~1/100, M_H~1/1000, C_{Na0}~C_0/2 then at say T=623 K, V >> 0.26 V so this inequality is also easily met in practice. Hence the quasi-stationary approximation remains valid for both profiles.

References

1. M. Dussauze, T. Cremoux, F. Adamietz, V. Rodriguez, E. Fagin, G. Yang and T. Cardinal "Thermal poling of optical glasses: Mechanisms and second-order optical properties" Int. J. of Applied Glass Science **3** 309-320 (2012)
2. H. An and S. Fleming "Second-order nonlinearity in thermally poled borosilicate glass" Appl. Phys. Lett. **89** 181111 (2006)
3. H. An and S. Fleming "Second-order optical nonlinearity and accompanying near-surface structural modifications in thermally poled soda-lime silicate glasses." J. Opt. Soc. Am. B **23** 2303-2309 (2006)
4. H. An and S. Fleming "Near-anode phase separation in thermally poled soda lime glass" Appl. Phys. Lett. **88** 181106 (2006)
5. M. Dussauze, V. Rodriguez, A. Lipovskii, M. Petrov, C. Smith, K. Richardson, T. Cardinal, E. Fargin and E. I. Kamisos "How does poling affect the structure of soda-lime glass?" J. Phys. Chem. C **114** 12754-12759 (2010)
6. T. Kaneko T "A diffusion technique for producing an inside-maximum distribution of refractive index in glass plates" Opt. Comm. **52** 17-23 (1984)
7. A.L.R. Brennand and J.S. Wilkinson "Planar waveguides in multicomponent glasses fabricated by field-driven differential drift of cations." Opt. Lett. **27** 906-908 (2002)
8. K. Liu and E.Y.B. Pun "Buried ion-exchanged glass waveguides using field assisted annealing." IEEE Photonics Technology Letters **17** 76-78 (2005)
9. W. Margulis and F. Laurell "Fabrication of waveguides in glasses by a poling procedure" Appl. Phys. Lett. **71** 2418-2420 (1997)
10. I.C.S. Carvalho, M Fokine, C.M.B. Cordeiro, H Carvalho and R. Kashyap "Borosilicate glass for photonic applications." Opt. Mat. **30** 1816-1821 (2008)

11. V Zhurikhina, Z Sadrieva , A Lipovskii, “Single-mode channel optical waveguides formed by the glass poling” , Optik, **137**, 203-208 (2017)

12. A. Lipovskii , V.V. Rusan and D.K. Tagantsev “Imprinting phase/amplitude patterns in glasses with thermal poling.” Solid State Ionics **181** 849-855 (2010)

13. L.A.H. Fleming, D.M. Goldie and A. Abdolvand “Imprinting of glass” Opt. Mat. Express **5** 1674-1681 (2015)

14. P.N. Brunkov, V.G. Melekhin, V.V. Goncharov, A.A. Lipovskii and M.I. Petrov “Submicron-Resolved Relief Formation in Poled Glasses and Glass-Metal Nanocomposites” Tech. Phys. Lett. **34** 1030-1033 (2008)

15. A.V. Redkov, V.G. Melehin, V.V. Statcenko and A.A. Lipovskii “Nanoprofiling of alkali-silicate glasses by thermal poling” J. Non-Cry. Solids. **409** 166-169 (2015)

16. R. Mariappan and B. Roling, “Investigation of bioglass-electrode interfaces after thermal poling”, Solid State Ionics **179** 671-677 (2008)

17. C.R. Mariappan and B. Roling “Mechanism and Kinetics of Na+ ion depletion under the anode during electro-thermal poling of a bioactive glass”, J. Non-Cryst. Solids. **356** 720-724 (2010)

18. J. Zakel, V. Heddinga, S.O. Steinmuller and B. Roling “Investigation of sodium ion depletion layers in electrothemally poled bioglasses by combining impedance spectroscopy and ToF-SIMS depth profiling”, Solid State Ionics **237** 46-49 (2013)

19. J. Zakel, M. Balabajew and B. Roling “On the mechanism of field-induced mixed ionic-electronic transport during electro-thermal poling of a bioactive sodium-calcium phosphosilicate glass”, Solid State Ionics **265** 1-6 (2014).

20. A. Lepicard, T. Cardinal, E. Fargin, F. Adamietz, V. Rodriguez, K. Richardson and M. Dussauze “Surface Reactivity control of a borosilicate glass using thermal poling” J. Phys. Chem. C **119** 22999-23007 (2015)

21. R. Oven and P.R. Young "Microwave loss of coplanar waveguides on electrically ion depleted borosilicate glass." IEEE Microwave and Wireless component Letters **15** 125-127 (2005)

22. D.E. Carlson "Ion depletion of glass at a blocking anode: 1, Theory and Experimental Results for alkali silicate glasses." J. Am. Ceram. Soc. **57** 291-294 (1974)

23. D.E. Carlson, K.W. Hang and G.F. Stockdale "Ion depletion of glass at a blocking anode: 2, Properties of ion depleted glass." J. Am. Ceram. Soc. **57,** 295-300 (1974)

24. D.E. Carlson "Anodic proton injection in glasses." J. Am. Ceram. Soc. **57**, 461-466 (1974)

25. M. I. Petrov, Ya. A. Lepen'kin, and A. A. Lipovskii "Polarization of glass containing fast and slow ions" J. of Appl. Phys. **112**, 043101 (2012)

26. R. Oven "Measurement of planar refractive index profiles with rapid variations in glass using interferometry and total variation regularized differentiation" J. Mod. Opt. **62**, S59-S66, (2015).

27. X. Prieto and J. Linares, "Increasing resistivity effects in field-assisted ion exchange for planar optical waveguide fabrication" Opt. Lett. **21** 1363 (1996)

28. A. N. Miliou, R. Srivastava and R.V. Ramaswamy, "Modeling of the index change in K^+-Na^+ ion-exchanged glass" Appl. Opt. **30** 674-681 (1991)

29. H Ikeda, D Sakai, S Funatsu, K Yamamoto, T Suzuki, K Harada and J Nishii1″Generation of alkali-free and high-proton concentration layer in a soda lime glass using non-contact corona discharge″ J of Appl. Phys. **114,** 063303 (2013)

30. K Kawaguchi, H Ikeda, D Sakai, S Funatsub, K Uraji, K Yamamoto, T Suzukic, K Harada, J Nishii "Accelerated formation of sodium depletion layer on soda lime glass surface by corona discharge treatment in hydrogen atmosphere" Appl. Surf. Sci. **300** 149–153 (2014)

31. M. Abou el Leil and A. R. Cooper, “Analysis of field assisted binary ion exchange” J. Am. Ceram. Soc. **62**, 390-395 (1979)

32. R. Oven, D. G. Ashworth and M. C. Page, “On the analysis of field-assisted ion diffusion into glass” J. Phys. (C): **4** (16), 4089 (1992)

33. R. Oven “Measurement of the refractive index of electrically poled soda-lime glass layers using leaky modes” Appl. Opt. **55** (32). 9123-9130 (2016).

34. R. Oven “AC impedance of poled glass during de-poling” Solid State Ionics **315** 14-18 (2018)

35. A.V.Anan`ev, A.A.Lipovskii and D.K.Tagantsev “Is frozen space charge responsible for SHG in poled silicate glasses only?” J. Non-Cryst. Solids. **458** 118-120 (2017)

FIGURE CAPTIONS

fig.1 Field assisted diffusion – first order model ignoring diffusion effects. Diffusion fronts indicated by dotted lines. (Colour on-line)

fig. 2 Comparison between analytical model and computer simulations. Parameters used are C_O= 6.8x10^{27}m^{-3}, C_{NaO}/C_O=0.605, C_{KO}/C_O =0.395, T= 400^{o}C, μ_{Na}=1.3x10^{-15} m^{2}V^{-1}s^{-1}, M_K=0.0125, M_H=0.001, V=150V and W=1 mm, t=3 hours. Concentrations normalized with respect to Co. For computer simulation ε_r= 5 was assumed. (Colour on-line)

fig. 3 Comparison between analytical model and computer simulations. V=100V and t=30 min other parameters as for fig. 2 (colour on-line). Concentrations normalized with respect to Co.

fig. 4.Comparison between analytical model and computer simulations for current density, time data. Parameters same as for fig. 2. Analytical is solid curve, dots are computer simulation. (Colour on-line)